Article

Solid-State NMR Study of MCM-41-type Mesoporous Silica Nanoparticles

Julien Trbosc, Jerzy W. Wiench, Seong Huh, Victor S.-Y. Lin, and Marek Pruski

J. Am. Chem. Soc., **2005**, 127 (9), 3057-3068• DOI: 10.1021/ja043567e • Publication Date (Web): 11 February 2005

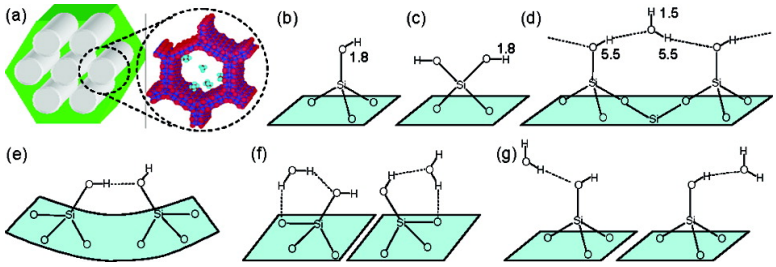

More About This Article

Additional resources and features associated with this article are available within the HTML version:

- Supporting Information
- Links to the 19 articles that cite this article, as of the time of this article download
- Access to high resolution figures
- Links to articles and content related to this article
- Copyright permission to reproduce figures and/or text from this article

View the Full Text HTML

J|A|C|S
ARTICLES
Published on Web 02/11/2005

Solid-State NMR Study of MCM-41-type Mesoporous Silica Nanoparticles

Julien Trébosc,[†] Jerzy W. Wiench,[†] Seong Huh,[†,‡] Victor S.-Y. Lin,[†,‡] and Marek Pruski*,[†]

Contribution from the Ames Laboratory and Department of Chemistry, Iowa State University, Ames, Iowa 50011-3020

Received October 22, 2004; E-mail: mpruski@iastate.edu

Abstract: A systematic study of the surface of MCM-41-type mesoporous silica nanoparticles prepared under low surfactant concentration was carried out using high-resolution solid-state nuclear magnetic resonance spectroscopy. The structures and concentrations of various species present during dehydration and rehydration of mesoporous silicas between −25 and 500 °C were detailed by employing one-dimensional and two-dimensional ^{1}H, ^{13}C, and ^{29}Si NMR, including ^{1}H signal intensity measurements, ^{1}H−^{1}H homonuclear correlation experiments (double quantum, exchange, and RFDR), and ^{1}H−^{29}Si heteronuclear correlation NMR. These experiments employed high MAS rates of up to 45 kHz. The study shows that the surfactant (CTAB) was almost completely removed by acid extraction. The residual molecules assumed prone positions along the pores, with the tailgroup being most mobile. The weakly adsorbed water was hydrogen bonded to the silanol groups, all of which were involved in such bonds under ambient humidity. Specific structures involving water and silanol groups were proposed for various stages of thermal treatment, which included dehydration, dehydroxylation, and subsequent rehydration.

1. Introduction

We recently reported a synthetic strategy geared toward developing a new generation of single-site catalysts supported on mesoporous silicas. It involves multifunctionalization of these materials via co-condensation, which provides control of the pore and particle morphology and, most importantly, allows for selective immobilization of a variety of catalytic groups inside the mesopores. Solid-state NMR spectroscopy plays a key role in characterization of these materials. Initially, MAS NMR of ^{1}H, ^{13}C, and ^{29}Si were used to provide direct information about the structure, relative concentration, location, and reactivity of various anchored groups in functionalized MCM-41 silicas.[1−4] Exploratory two-dimensional ^{1}H−^{13}C NMR experiments were performed in order to detail the location of these groups with respect to each other and the silica support.[5]

Proper understanding of such surfaces cannot be achieved without a thorough knowledge of the structure of pure MCM supports under the relevant conditions. While excellent NMR studies of several types of silicas have been reported,[6−15] uncertainties regarding the interpretation of ^{1}H spectra in such systems exist. These complex surfaces exhibit a variety of silicon sites, Si−O−Si bond angles, and hydrogen bond properties, which all vary with the preparation method and sample treatment. In addition, the organically functionalized MCM-41 materials cannot be subjected to severe calcination, and even when used as catalysts may exhibit new characteristics of "as-synthesized" samples. We will refer to these materials as MCM-41-type mesoporous silica nanoparticles (MSNs). The newest advancements in solid-state NMR, in particular, ultrafast magic angle spinning (MAS), provide improved tools for such investigations. By employing MAS rates approaching 45 kHz, we obtained high-resolution ^{1}H spectra of MCM-41 surfaces in a routine fashion without the necessity of using multiple pulse sequences for homonuclear decoupling. This, in turn, opened the possibility of using ^{1}H−^{1}H homonuclear correlation methods, including 2D exchange, RFDR, and double quantum (DQ) ^{1}H−^{1}H MAS NMR, as well as heteronuclear correlation (HETCOR) NMR to gain additional insights. In the present

[†] Ames Laboratory.
[‡] Department of Chemistry.

(1) Huh, S.; Wiench, J. W.; Trewyn, B. G.; Song, S.; Pruski, M.; Lin, V. S. Y. *Chem. Commun.* **2003**, 2364−2365.
(2) Huh, S.; Wiench, J. W.; Yoo, J.-C.; Pruski, M.; Lin, V. S. Y. *Chem. Mater.* **2003**, *15*, 4247−4256.
(3) Lin, V. S. Y.; Radu, D. R.; Han, M.-K.; Deng, W.; Kuroki, S.; Shanks, B. H.; Pruski, M. *J. Am. Chem. Soc.* **2002**, *124*, 9040−9041.
(4) Radu, D. R.; Lai, C.-Y.; Wiench, J. W.; Pruski, M.; Lin, V. S. Y. *J. Am. Chem. Soc.* **2004**, *126*, 1640−1641.
(5) Trebosc, J.; Wiench, J. W.; Huh, S.; Lin, V. S. Y.; Pruski, M. In preparation.
(6) Bronnimann, C. E.; Ziegler, R. C.; Maciel, G. E. *J. Am. Chem. Soc.* **1988**, *110*, 2023−2026.
(7) Liu, C. C.; Maciel, G. E. *J. Am. Chem. Soc.* **1996**, *118*, 5103−5119.
(8) Alam, T. M.; Fan, H. *Macromol. Chem. Phys.* **2003**, *204*, 2023−2030.
(9) d'Espinose de la Caillerie, J.-B.; Aimeur, M. R.; El Kortobi, Y.; Legrand, A. P. *J. Colloid Interface Sci.* **1997**, *194*, 434−439.
(10) Ek, S.; Root, A.; Peussa, M.; Niinisto, L. *Thermochim. Acta* **2001**, *379*, 201−212.
(11) Turov, V. V.; Leboda, R. *Adv. Colloid Interface Sci.* **1999**, *79*, 173−211.
(12) Maciel, G. E. In *Solid-State NMR Spectroscopy of Inorganic Materials*; Fitzgerald, J. J., Ed.; American Chemical Society: Washington, DC, 1999; pp 326−356.
(13) Christiansen, S. C.; Zhao, D.; Janicke, M. T.; Landry, C. C.; Stucky, G. D.; Chmelka, B. F. *J. Am. Chem. Soc.* **2001**, *123*, 4519−4529.
(14) Bronnimann, C. E.; Chuang, I.-S.; Hawkins, B. L.; Maciel, G. E. *J. Am. Chem. Soc.* **1987**, *109*, 1562−1564.
(15) Shenderovich, I. G.; Buntkowsky, G.; Schreiber, A.; Gedat, E.; Sharif, S.; Albrecht, J.; Golubev, N. S.; Findenegg, G. H.; Limbach, H.-H. *J. Phys. Chem. B* **2003**, *107*, 11924−11939.

study, we describe a pure MSN sample prepared under low surfactant concentration, in the presence of residual amounts of surfactant.

2. Experimental Section

2.1. Sample Synthesis. The material was synthesized according to our previous reports.[2,16] A mixture of cetyltrimethylammonium bromide surfactant ($CH_3(CH_2)_{15}N(CH_3)_3Br$, referred to as CTAB) (2.0 g, 5.49 mmol), 2.0 M NaOH (aq) (7.0 mL, 14.0 mmol), and H_2O (480 g, 26.67 mol) was heated at 80 °C for 30 min with a constant stirring (550 rpm). To this clear solution was added rapidly via injection TEOS (8.31 g, 39.9 mmol), yielding an opaque reaction mixture. The white solid products of synthesis were observed after vigorous (550 rpm) stirring of the mixture for ~2 min. The as-synthesized mesoporous material was obtained after an additional 2 h of heating at 80 °C, followed by hot filtration, washing with copious amounts of water and methanol, and drying under vacuum. An acid extraction of the CTAB surfactant was performed at 60 °C by placing 1.0 g of the as-synthesized MCM-41 silica in a mixture of methanol (100 mL) and concentrated hydrochloric acid (1.0 mL) for 6 h. The silica was then filtered, washed with water and methanol, and dried under vacuum for 3 h at 90 °C. The resulting material had the BET surface area of 750 m^2/g and the pore diameter of 2.5 nm. It was then exposed to 55% humidity at 30 °C (sample **A**) and evacuated for 2 h under 10^{-5} atm at temperatures between 30 and 500 °C (these samples will be referred to as **A30** through **A500**, or series **A**). Another series of silicas (**B**) was prepared after rehydrating sample **A500** in steam of boiling water under atmospheric pressure for 3 min. The steaming process, which yielded sample **B** with weight increased by approximately 30%, was followed by evacuation at 30 °C for 45 min (sample **B30**) and evacuation at elevated temperatures for 2 h (samples **B100** through **B250**).

2.2. Solid-State NMR. Solid-state NMR experiments were performed at 9.4 T on a Chemagnetics Infinity spectrometer equipped with 5 (Chemagnetics), 3.2 (Chemagnetics), and 1.8 mm (A. Samoson[17−19]) double-tuned probes capable of MAS at 10, 25, and 50 kHz, respectively. The 3.2 mm probe was only used for ^{1}H signal intensity measurements and variable temperature (VT) ^{1}H MAS experiments on samples of series **B**. The samples were packed in the rotors and then dried successively at temperatures ranging from 30 to 500 °C for 2 h under 10^{-5} atm. The rotors were then tightly capped in a glovebag under dry nitrogen to avoid rehydration. Samples were fully equilibrated after each treatment, as evidenced by no changes in the observed spectra during the time of the experiments. A suite of one-dimensional (1D) and two-dimensional (2D) NMR was used, including 1D MAS (^{1}H, ^{29}Si), 2D ^{1}H−^{1}H double quantum (DQ) MAS, 2D ^{1}H−^{1}H exchange and RFDR NMR, 1D ^{13}C{^{1}H} and ^{29}Si{^{1}H} cross polarization (CP) MAS NMR, and 2D ^{1}H−^{29}Si heteronuclear correlation (HETCOR) NMR. In ^{1}H MAS experiments, the relaxation delay between accumulations was 4 s, as the typical T_1 values measured in our samples by using inversion recovery ranged between 0.4 and 0.75 s. In the 2D experiments, all of which involved ^{1}H excitation, the acquisition delay was reduced to 1 s. The hypercomplex method was employed to discriminate the sine and cosine parts in the F_1 domain of 2D spectra.

Listed below are other essential experimental parameters used in these experiments, where ν_R denotes the sample rotation rate, ν_{RF} the magnitudes of radio frequency field, NS the number of scans, and AT the total acquisition time of a 2D spectrum.

^{1}H MAS: $\nu_R = 0-47$ kHz; $\nu_{RF} = 170$ (1.8 mm probe) and 100 kHz (3.2 mm probe); NS = 64. The DEPTH pulse sequence was used for background suppression.[20] The sequence used an additional pair of 180° pulses and a phase cycling scheme designed to attenuate the probe ringing and the background ^{1}H signal from nuclei outside of the rotor.

^{1}H−^{1}H DQ MAS: $\nu_R = 40$ kHz; $\nu_{RF} = 170$ kHz. The back-to-back (BABA) sequence was selected for excitation and reconversion of DQ coherences due to its excellent performance under 40 kHz MAS.[21] Using a rotor-synchronized t_1 increment of 100 μs and NS = 16, 32, or 64 for BABA pulse train length of 100, 300, and 500 μs long, respectively, the acquisition times of 2D data were between 1 and 4 h.

^{1}H−^{1}H 2D exchange and RFDR: $\nu_R = 40$ kHz; $\nu_{RF} = 170$ kHz; NS = 8; t_1 increment = 200 μs; mixing times $\tau_m = 0$, 1, 10, 20, and 100 ms; AT = 1 h. In RFDR, one 180° pulse per rotor period was introduced during the mixing time.[22]

^{29}Si MAS: $\nu_R = 10$ kHz (5 mm probe); $\nu_{RF} = 15.6$ kHz; NS = 240; relaxation delay = 300 s; ν_{RF} (^{1}H) during CW decoupling = 55 kHz.

^{1}H−^{29}Si CP: ν_{RF} (^{1}H) during CP = 20 ± 5 kHz (ramped); NS = 640; relaxation delay = 2 s; other conditions were the same as in ^{29}Si MAS.

^{1}H−^{29}Si CP HETCOR: $\nu_R = 40$ kHz; ν_{RF} (^{29}Si) = 80 kHz; ν_{RF} (^{1}H) during CP = 120 ± 20 kHz (ramped), ν_{RF} (^{1}H) during CW decoupling = 10 kHz; NS = 2400; AT = 4 days.

All ^{1}H, ^{29}Si, and ^{13}C chemical shifts are reported using the δ scale and are referenced to tetramethylsilane (TMS) at 0 ppm. In Figures 5−7 and 10, the consecutive contours reflect a 2-fold change in the intensity. In most spectra, the lowest level corresponds to about 3% of the maximum intensity observed in a given series, whereas the skyline projections are normalized to the same height. In Figure 7, the floor is elevated due to the low signal-to-noise ratio.

The quantitative analysis of ^{1}H concentration was carried out by comparing the integrated NMR intensities at different hydration states with a calibrated reference sample and was additionally verified by monitoring the weight loss of the silica, as described in detail in section 3.2.

3. Results and Discussion

3.1. Ultrafast MAS NMR. The pursuit of higher sample rotation rates has led to the construction of probes capable of MAS at 40−70 kHz.[17−19] We have recently shown that a considerable improvement in resolution can be achieved in functionalized MSNs upon increasing the sample rotation rate from 10 to 45 kHz.[5] Further, high-speed MAS provides an easy, sensitive, and robust strategy for acquiring the high-resolution ^{1}H−^{1}H homonuclear spectra and ^{1}H−X (X = ^{29}Si and ^{13}C) heteronuclear NMR spectra in such samples.[5] As Figure 1 demonstrates, a similar improvement in resolution is achieved in nonfunctionalized MCM-41 silicas. The static ^{1}H NMR spectrum of sample **A**, at the bottom of Figure 1, can be roughly fitted by a superposition of two lines with 1.5 and 8 kHz line widths (fwhm). This relatively moderate broadening, which is mainly homogeneous due to ^{1}H−^{1}H dipolar interactions, was almost completely eliminated under MAS at 45 kHz. The resolution in this sample was not improved by combining MAS with multipulse sequences, such as FSLG.[23] Indeed, as will be shown later, the residual line width was controlled by the exchange processes and inhomogeneous broadening due to distribution of chemical shifts. The main artifact associated with this approach is the sample heating due to friction between the rotor and the surrounding air. By using the isotropic chemical

(16) Huh, S.; Chen, H.-T.; Wiench, J. W.; Pruski, M.; Lin, V. S. Y. *J. Am. Chem. Soc.* **2004**, *126*, 1010−1011.
(17) Samoson, A.; Tuherm, T.; Past, J.; Reinhold, A.; Anupõld, T.; Heinmaa, I. *Top. Curr. Chem.* **2004**, *246*, 15−31.
(18) Samoson, A. In *Encyclopedia of Nuclear Magnetic Resonance*; Grant, D. M., Harris, R. K., Eds.; John Wiley & Sons: Chichester, U.K., 2002; Vol. 9, pp 59−64.
(19) Samoson, A.; Tuherm, T.; Past, J. *Chem. Phys. Lett.* **2002**, *365*, 292−299.
(20) Cory, D. G.; Ritchey, W. M. *J. Magn. Reson.* **1988**, *80*, 128−132.
(21) Feike, M.; Demco, D. E.; Graf, R.; Gottwald, J.; Hafner, S.; Spiess, H. W. *J. Magn. Reson. A* **1996**, *122*, 214−221.
(22) Bennett, A. E.; Ok, J. H.; Griffin, R. G.; Vega, S. *J. Chem. Phys.* **1992**, *96*, 8624−8627.
(23) Bielecki, A.; Kolbert, A. C.; de Groot, H. J. M.; Griffin, R. G.; Levitt, M. H. *Adv. Magn. Reson.* **1990**, *14*, 111−124.

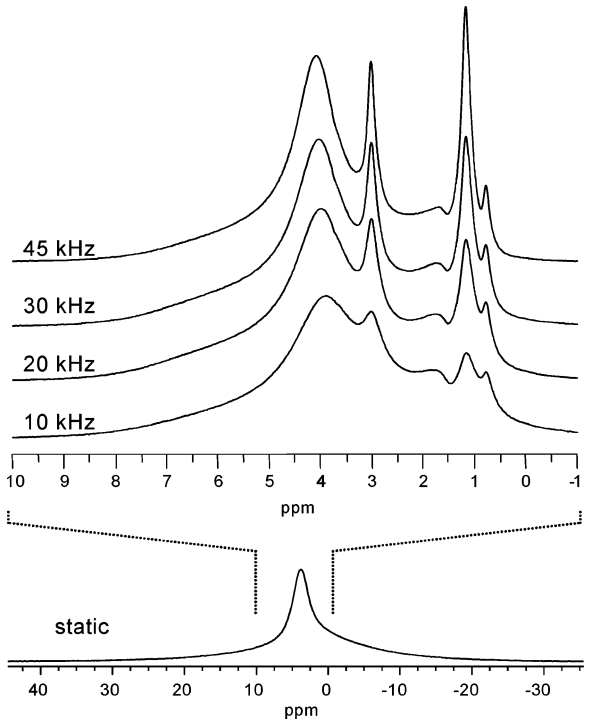

Figure 1. ^{1}H spectra of MCM-41-type nanoparticles acquired under static and MAS conditions as indicated in the figure. For fastest spinning rates, the spectrum exhibits mainly inhomogeneous and/or exchange broadening.

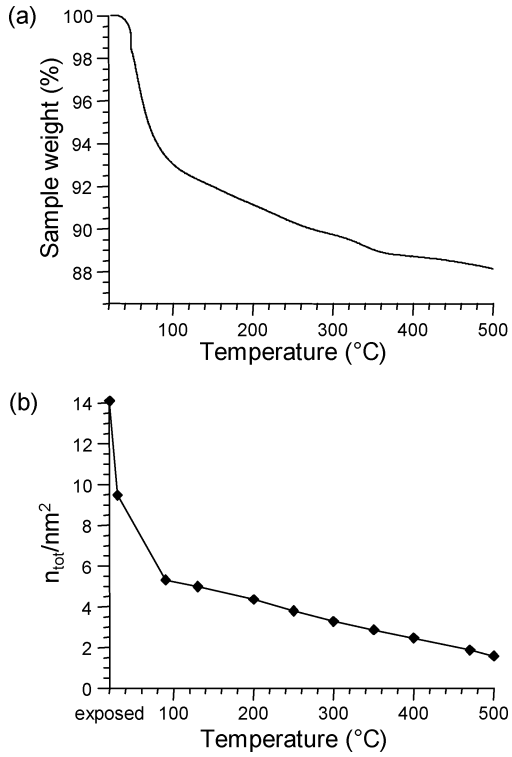

Figure 2. Results of TGA (a) and ^{1}H signal intensity measurements (b) for sample **A**. The initial water content was not identical in both measurements due to different ambient conditions in the laboratories.

shift of ^{207}Pb in lead nitrite as a thermometer,[24] we have determined that the rotor temperature increased by 10 to 15 °C above the ambient under 40 kHz MAS. In the present study, we made no effort to neutralize this effect.

We note that in strongly coupled systems of ^{1}H spins, the complete line narrowing cannot be achieved by 40 kHz MAS alone. For example, a 2D exchange spectrum of glycine, acquired with $\tau_m = 0$ under 40 kHz MAS,[25] exhibited 1 kHz wide patterns typical of homogeneously broadened lines in strongly coupled spin systems.

3.2. TGA and Quantitative Measurement of ^{1}H Concentration. The results of thermogravimetric analysis (TGA) and ^{1}H NMR signal intensity measurement in sample **A** are shown in Figure 2. The TGA analysis (Figure 2a) was performed on a TA instruments TGA 2950 thermogravimetric analyzer with a temperature ramp of 5 °C/min under continuous flow of nitrogen (100 mL/min).

Since the exact knowledge of the concentration of various hydrogen species was essential for the interpretation of NMR spectra, the ^{1}H signal intensity was determined in two independent experiments using 3.2 and 1.8 mm rotors, which were spun at 20 and 40 kHz, respectively. Approximately 10 mg of sample **A** was loaded into the rotors and measured in a hydrated state and after 2 h of evacuation at 30, 90, 130, 200, 250, 300, 350, 400, 470, and 500 °C. The absolute intensities were referenced to carefully weighed samples of adamantane, which were diluted with NMR-silent powder (sulfur) to roughly match the hydrogen content of the MSNs. The reference samples were measured using a delay of 10 s between scans, which allowed for full recovery of their equilibrium magnetization, under otherwise identical conditions. Since the intensities observed using different probes agreed to within 10% at all temperatures, the average values were used throughout this work. These measurements were further confirmed by monitoring the weight loss of the samples after each thermal treatment.

Table 1. ^{1}H NMR Signal Intensities Measured in Sample **A**

			Individual Peaks[a]					
sample	n_{tot}[a]	n_H[a]	3–5 ppm[a]	1.8 ppm[a]	wide base[a]	CTAB[a]	CTAB[b]	n_{OH}[a,c]
A	14.1	11.9	11.7	0.0	0.2	2.2	5.2	4.0
A30	9.5	7.5	5.8	0.3	1.3	2.2	5.2	
A90	5.3	3.6	0.9	0.9	1.7	1.7	4.1	
A130	5.0	3.2	0.2	1.3	1.6	1.8	4.3	
A200	4.3	3.0	0.1	1.2	1.7	1.4	3.3	
A250	3.8	2.9	0.1	1.4	1.5	0.8	2.0	
A300	3.3	2.8	0.0	1.4	1.4	0.5	1.1	
A350	2.8	2.8	0.0	1.6	1.2	0.05	0.1	2.3
A400	2.4	2.4	0.0	1.5	0.9	0.05	0.1	
A470	1.9	1.9	0.0	1.2	0.7	0.0	0.0	
A500	1.6	1.6	0.0	1.0	0.6	0.0	0.0	1.7

[a] Number of hydrogen atoms/nm^2. [b] Number of molecules/100 nm^2. [c] From ^{29}Si NMR.

The results of ^{1}H signal intensity measurements are listed in Table 1, which includes the total hydrogen concentration per nm^2 of the silica surface (n_{tot}) (also shown Figure 2b) and the concentration of hydrogen (n_H) exclusive of the intensities due to CTAB. Also listed in Table 1 are the specific contributions from the major resonances observed in the ^{1}H MAS spectra, including the resonances at 3−5 and 1.8 ppm, the peaks representing CTAB, and the wide resonance distributed between 2 and 8 ppm. The individual intensities were obtained by deconvolution of the spectra obtained under 40 kHz MAS because they were better resolved (see Figure 1). Since the resonance between 2 and 8 ppm could not be approximated by a single Gaussian or Lorentzian line and was susceptible to

(24) Bielecki, A.; Burum, D. P. *J. Magn. Reson. A* **1995**, *116*, 215−220.
(25) See Supporting Information for details.

Table 2. ^{1}H Chemical Shift of Water Molecules Found in Various Environments Related to This Work

species	δ_{CS}[a]	conditions	ref
H_2O monomeric	1.0	H_2O diluted in CCl_4	26
	1.2	H_2O diluted in $CHCl_3$	26
	0.3−0.4	H_2O in C_6D_6 (−20 to 50 °C)	27
	1.0−1.1	H_2O in CCl_4 (−40 to 35 °C)	27
	1.6−1.9	H_2O in $CDCl_3$ (−40 to 35 °C)	27
	0.5	H_2O gaseous	28, 29
H_2O cluster	5.3−5.5	H_2O in C_6D_6 (0 to 18 °C)	29
	4.7−5.0	H_2O bulk (0 to 30 °C)	30
	4.8−5.2	H_2O in CCl_4 (−20 to 8 °C)	30
	4.1−5.1	PC in H_2O (1 to 49 °C)	30
H_2O surface	3.9−5.0	H_2O on surfaces of titania/silica (−50 to 50 °C)	31
	4.5−5.6	H_2O on surfaces of silicates (−50 to 60 °C)	32
H_2O ice	7.7 ± 1	ice (−90 °C)	33
	7.0 ± 0.5	ice (−50 to −135 °C)	34
	7.8	ice, single crystal (−80 °C)	35
	7.9	ice (−80 °C)	36

[a] In parts per million with respect to TMS.

Table 3. ^{1}H NMR Signal Intensities Measured in Sample **B**

sample	n_H[a]	3–5 ppm[a]	1.8 ppm[a]	wide base[a]	n_{OH}[a,b]
B	28	25	0	3.0	1.7
B30	5.4	1.8	0.7	2.9	*c*
B250	1.8	∼0	1.0	0.8	*c*

[a] Number of hydrogen atoms/nm^2. [b] From ^{29}Si NMR. [c] Not measured.

baseline distortions, steps were taken to ensure the best possible reliability of the fits. The data reported for this peak were approximated by subtracting the intensities of the well-resolved resonances from the total intensity of the spectrum. Similar results were obtained by using a superposition of several lines to fit the distributed resonance. Still, these difficulties caused the reliability of the spectral intensities corresponding to the distributed resonance to be estimated to within 0.5 H atoms/nm^2. Other resonances were estimated to within 10%. The last column in Table 1 shows the concentration of OH groups, n_{OH}, which was estimated from the ^{29}Si NMR spectra.[25] In sample **A**, these spectra yielded the relative concentrations of Q^2 and Q^3 silicon sites associated with geminal $(-O-)_2Si(OH)_2$ and single $(-O-)_3SiOH$ silanol groups of 2 and 28%, respectively. In sample **A500**, the corresponding numbers dropped to 1.5% and 12%. Clearly, the single SiOH groups are the dominant silanol species in these materials. The n_{OH} values were estimated with an accuracy of ±0.5.

As expected, the most significant weight loss is observed for samples treated at the lower temperatures, owing to the removal of adsorbed water. The TGA and NMR curves show essentially parallel behavior at temperatures above 100 °C. The higher initial rate of decrease in signal intensity observed by NMR is due to prolonged evacuation at each temperature. At temperatures above 130 °C, the weight loss is mainly due to dehydroxylation. The ^{1}H intensity measurements were also carried out with the rehydrated sample **B**. These results are shown in Table 3 and discussed in section 3.3.2.d.

3.3. Interpretation of ^{1}H Spectra. Several 1D and 2D experiments were performed on sample series **A** and **B** after each treatment under fast MAS. Only the most representative spectra relevant to the discussion below are shown in Figures 3−7, 9−11, and in the Supporting Information.[25] Also shown, in Figure 8, are the structures of surface OH groups and water

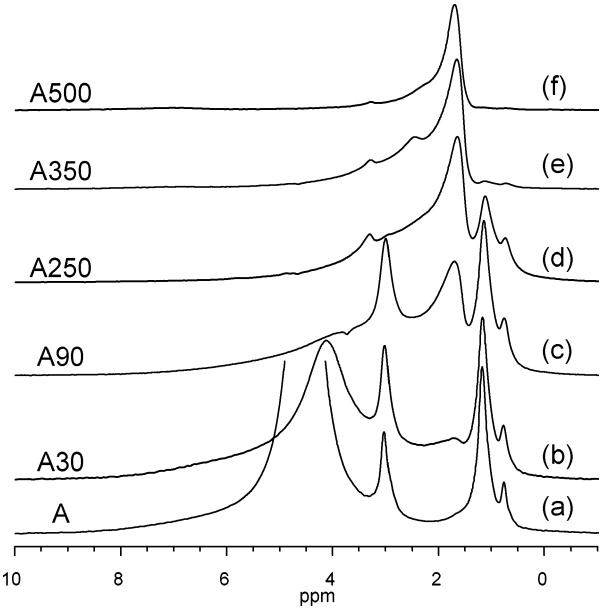

Figure 3. ^{1}H NMR spectra of samples **A** (a), **A30** (b), **A90** (c), **A250** (d), **A350** (e), and **A500** (f) under 40 kHz MAS.

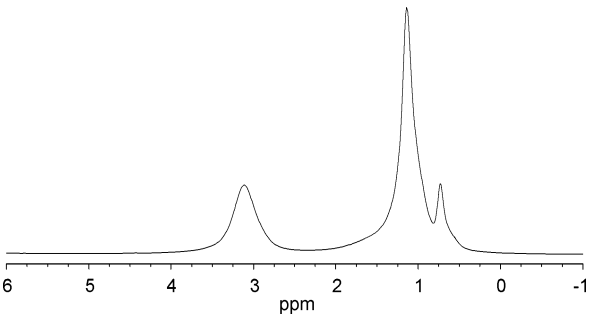

Figure 4. ^{1}H NMR spectrum of templated MCM-41 sample with CTAB filling the mesopores acquired under 40 kHz MAS.

in several configurations considered in this work. Table 2 includes the chemical shifts reported in the literature for water in various hydrogen-bonded environments.[26−36]

3.3.1. CTAB. The high shielded region of spectra a−d in Figure 3 included three well-resolved peaks at 0.8, 1.2, and 3.1 ppm. On the basis of the ^{1}H MAS spectra of CTAB $(CH_3(CH_2)_{15}N(CH_3)_3Br)$ in solution (not shown) and the templated MCM-41 sample (shown in Figure 4), we assigned these resonances to $-CH_3$, $-CH_2-$, and $-CH_2-N(CH_3)_3$ protons in the residual surfactant molecules scattered inside the mesopores. Similar results were reported earlier in mesoporous silicas by Christiansen et al.[13] and Camus et al.[37] This assignment is in

(26) Cohen, A. D.; Reid, C. *J. Chem. Phys.* **1956**, *25*, 790−791.
(27) Nakahara, M.; Wakai, C. *Chem. Lett.* **1992**, 809−812.
(28) Schneider, W. G.; Bernstein, H. J.; Pople, J. A. *J. Chem. Phys.* **1958**, *28*, 601−607.
(29) Hindman, J. C. *J. Chem. Phys.* **1966**, *44*, 4582−4592.
(30) Cogley, D. R.; Falk, M.; Butler, J. N.; Grunwald, E. *J. Phys. Chem.* **1972**, *76*, 855−864.
(31) Gun'ko, V. M.; Zarko, V. I.; Turov, V. V.; Voronin, E. F.; Tischenko, V. A.; Chuiko, A. A. *Langmuir* **1995**, *11*, 2115−2120.
(32) Turov, V. V.; Chodorowski, S.; Leboda, R.; Skubiszewska-Zieba, J.; Brei, V. V. *Colloids Surf. A* **1999**, *158*, 363−373.
(33) Pines, A.; Ruben, D. J.; Vega, S.; Mehring, M. *Phys. Rev. Lett.* **1976**, *36*, 110−113.
(34) Kinney, D. R.; Chuang, I.-S.; Maciel, G. E. *J. Am. Chem. Soc.* **1993**, *115*, 6786−6794.
(35) Rhim, W. K.; Burum, D. P.; Elleman, D. D. *J. Chem. Phys.* **1979**, *71*, 3139−3141.
(36) Burum, D. P.; Rhim, W. K. *J. Chem. Phys.* **1979**, *70*, 3553−3554.

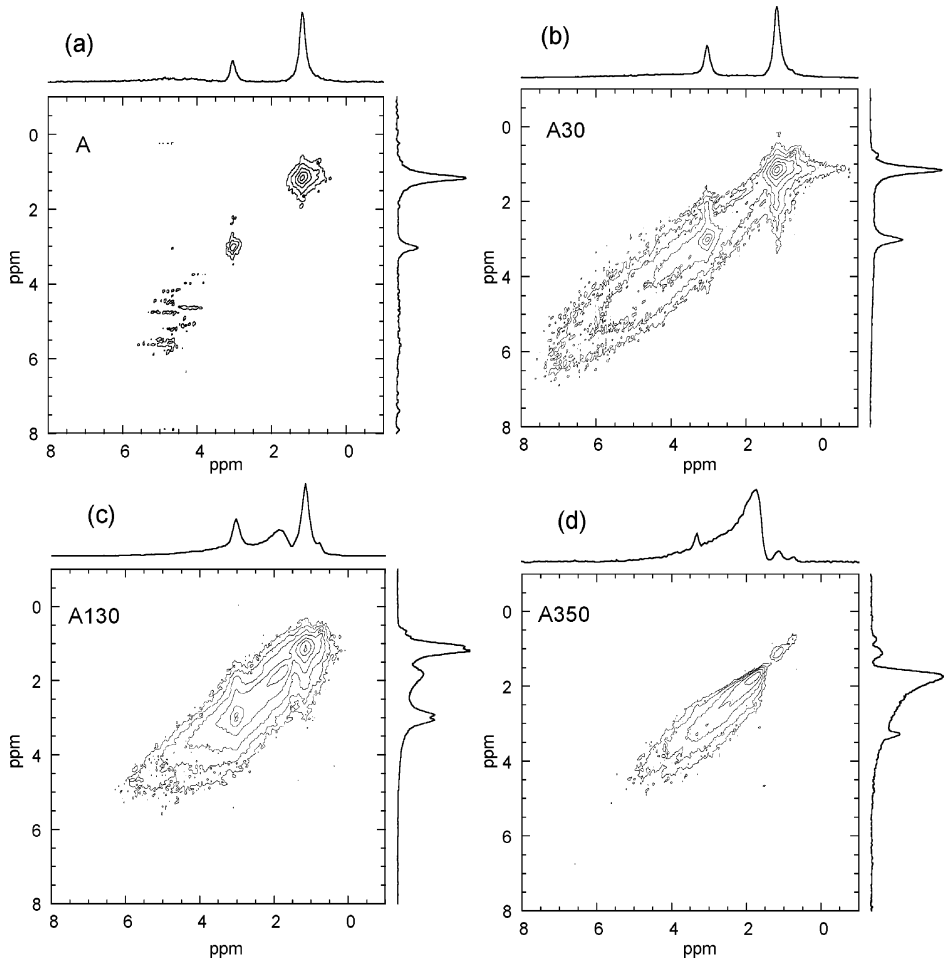

Figure 5. $^{1}H-^{1}H$ DQ MAS NMR spectra of sample **A** (a), **A30** (b), **A130** (c), and **A350** (d). For details, see the Experimental Section.

agreement with several other observations. First, the positions of these resonances were unaffected by the thermal treatment. Second, their intensities were strongly reduced by the treatments between 200 and 300 °C, and essentially eliminated after calcination at 350 °C (see Table 1), which concurs with the TGA analysis of a templated sample (not shown). Third, these resonances did not reappear upon subsequent rehydration. Finally, the presence of carbon in sample **A30** was confirmed by $^{1}H-^{13}C$ CPMAS experiment, in which the resonances representing CTAB were clearly identified.[25] On the basis of the ^{1}H signal intensities, the concentration of CTAB in sample **A** was estimated at 1 molecule/3 nm of channel length, which corresponded to 3.5 ± 0.5% of the initial amount in the templated sample.

The 1D and 2D ^{1}H NMR spectra provided additional details about the conformation and dynamics of these molecules. The DQ-filtered spectra of samples **A**, **A30**, and **A130** in Figure 5 include the intense diagonal resonances due to CTAB, especially at short excitation times. Since the DQ coherences are generated via the homonuclear dipole−dipole coupling between protons,[22] this demonstrates that relatively strong $^{1}H-^{1}H$ interactions are present within the CTAB's headgroup ($-N(CH_3)_3$), the CH_2 groups, and to a much lesser extent, within the tailgroup (CH_3). Thus, the surfactant molecules that remained in sample **A** after the extraction are relatively rigid in comparison with other moieties containing hydrogen. In samples **A30** and **A130**, the strong cross-peaks were also observed between the protons in the headgroup and the adjacent CH_2 groups. Furthermore, these groups exhibit connectivities with the surface OH groups and water, as evidenced by the weak vertical ridges in DQ spectra of Figure 5b,c. Strong cross-peaks between these species were also observed in the 2D exchange spectra shown Figure 6b,d,f. Note that these spectra were taken with $\tau_m = 100$ ms, which permitted long-range redistribution of magnetization due to spin diffusion, even under 40 kHz MAS. However, weak cross-peaks between CTAB and surface species were observed at values of τ_m as short as 1 ms.[25] Finally, clear evidence of the proximity of the headgroup and the CH_2 groups in CTAB to the silica surface is found in the $^{1}H-^{29}Si$ HETCOR spectrum of Figure 7. The cross sections corresponding to Q^3 and Q^4 shown at the bottom of Figure 7 indicate that the CH_2 groups correlate mainly with Q^4 sites, which is consistent with their hydrophobic character. The tailgroup in CTAB appears to be more mobile, as the peak at 0.8 ppm is undersized at short excitation times and does not correlate with other resonances in the DQ MAS and $^{1}H-^{29}Si$ HETCOR spectra. These results strongly suggest that the CTAB molecules reside in the prone position along the channel walls. We finally note that the resonance at 3.1 ppm was essentially eliminated from spectrum (d) in Figure 3, while those at 0.8 and 1.2 ppm were still present. This indicates that CTAB has decomposed at around 250 °C and that its head section was removed first.

(37) Camus, L.; Goletto, V.; Maquet, J.; Gervais, C.; Bonhomme, C.; Babonneau, F.; Massiot, D. *J. Sol-Gel Sci. Technol.* **2003**, *26*, 311−314.

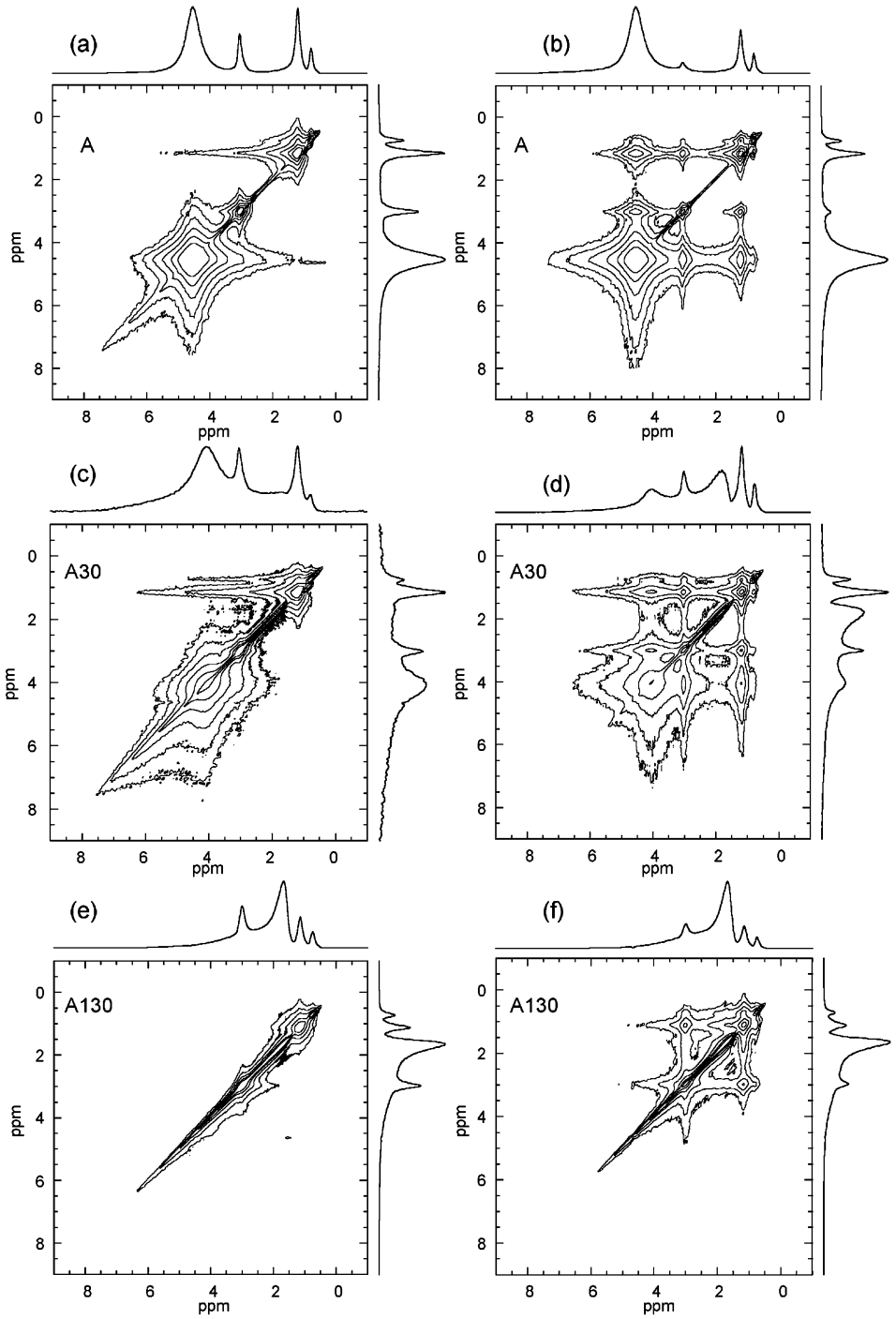

Figure 6. Two-dimensional exchange $^1H-^1H$ correlation spectra under 40 kHz MAS: (a) sample **A** with $\tau_m = 0$ ms; (b) sample **A** with $\tau_m = 100$ ms; (c) sample **A30** with $\tau_m = 0$ ms; (d) sample **A30** with $\tau_m = 100$ ms; (e) sample **A130** with $\tau_m = 0$ ms; and (f) sample **A130** with $\tau_m = 100$ ms.

3.3.2. Water and Silanol Groups. 3.3.2.a. Room Temperature (Samples A and A30). The presence of water has a dominant effect on the ^1H NMR spectra of the MSNs. The samples exposed to high humidity, for example, during steaming, exhibited a strong resonance at 4.8 ppm representing mostly weakly bound, relatively mobile water.[25] Sample **A**, exposed to 55% relative humidity at 25 °C, exhibits a less intense resonance at around 4.5 ppm (Figure 3a). As expected, this resonance could not be observed in the DQ MAS NMR spectrum of Figure 5a, due to motional averaging of the dipolar coupling between neighboring protons. However, it was observed in the conventional 2D exchange spectrum with a mixing time of $\tau_m = 0$ (shown in Figure 6a). The width of this spectrum measured along the direction perpendicular to the diagonal corresponds to the residual homogeneous broadening under 40 kHz MAS. At 4.5 ppm, this broadening is Lorentzian with the fwhm = 300 Hz and is due to the residual homonuclear coupling and the exchange processes to be discussed later.

The MAS, DQ MAS, and 2D exchange spectra of sample **A30** are shown in Figures 3b, 5b, and 6c,d. After 2 h evacuation, a significant amount of the adsorbed water was removed, as the peak at 4.5 ppm, which dominated the spectrum of the hydrated sample, has decreased in intensity by $^1/_2$ (see Figure 2b and Table 1) and shifted in the upfield direction to 4.1 ppm.

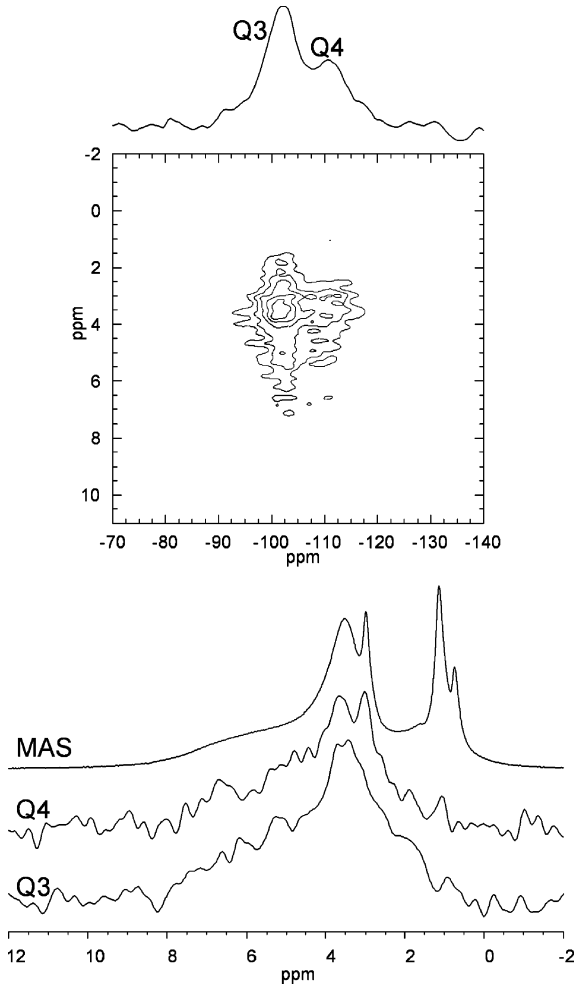

Figure 7. Two-dimensional $^{1}H-^{29}Si$ CP HETCOR spectrum of MCM-41 sample **A30** taken under 40 kHz MAS. For details, see the Experimental Section. ^{1}H traces below the 2D spectrum represent, from top to bottom, the 1D MAS spectrum of the same sample and the ^{1}H spectra correlated to Q^4 and Q^3 silicon sites.

Note that the only additional features observed in the MAS spectra of samples **A** and **A30** (Figure 3a,b) are the previously discussed peaks representing CTAB and a residual broad base between 2 and 7 ppm. In Figure 6a−d, this base appears as a narrow diagonal ridge, which proves that the line broadening involved is mainly inhomogeneous (distributed) under fast MAS. The DQ-filtered spectrum of sample **A30** (Figure 5b) also exhibits a weak wide ridge along the diagonal, in addition to the peaks attributed to CTAB. This result is consistent with greater than before rigidity of the contributing spins, which becomes increasingly apparent upon further thermal treatment. The isolated, that is, non-hydrogen bonded, single and/or geminal SiOH groups were not detected directly at their usual position around 1.8 ppm[6,9,14,38] in the spectrum of Figure 3a. A small peak at 1.8 ppm begun to emerge in sample **A30** (Figure 3b) and became dominant at higher temperatures.

Although similar spectral features were observed in previous studies, the individual structures of surface species on silicas are not well understood. The intense resonance in the 3−5 ppm range was earlier reported in other silicas at early stages of hydration. By using the CRAMPS,[39] Liu and Maciel[7] observed a peak at 4.1 ppm in humidified fumed silica (Cab−O−Sil), which they attributed to water molecules in fast exchange between liquid and physically adsorbed states. The untreated (i.e., not humidified) sample yielded a resonance at 3.5 ppm assigned to physisorbed water, which could be easily desorbed by evacuation at 25 °C. The evacuation at 100 °C led to further decrease in the intensity of this resonance, which shifted to 3 ppm and was assigned to "rapidly exchanging weakly hydrogen-bonded hydroxyls, including those of both water and silanols". As the water was being removed, the intensity of the resonance at 1.8 ppm representing non-hydrogen-bonded silanols increased. ^{1}H MAS NMR study of dehydration and rehydration of fumed silicas (Cab−O−Sil and Aerosil 200) was also reported by De la Caillerie et al.,[9] who assigned the resonance at around 2.7 ppm to strongly bound water which capped the silanol groups. They also concluded that at appropriately high water coverages, this proton population was in fast exchange with liquidlike water resonating at 5.8 ppm, yielding the resonances between 4.6 and 2.7 ppm depending on the water content. More recently, Grünberg et al.[40] studied the hydrogen bonding of water in a sample of MCM-41 which was calcined to 550 °C in order to remove the surfactant prior to rehydration. In that study, the peak at around 3 ppm was also attributed to fast exchange between silanol groups and hydrogen-bonded water molecules. The TGA and ^{1}H NMR investigation of silicalites by Turov et al. reported the chemical shift of water at around 5 ppm at room temperature.[32] Several other studies of silicas have also attributed the resonances at 4.5−5 ppm to water on strongly hydrated surfaces and those near 3 ppm to water on significantly dehydrated surfaces, as reviewed by Turov et al.[11]

Clearly, the resonance shift between 4.8 and 4.1 ppm observed in our MSN system is consistent with gradual elimination of the weakly adsorbed water. To propose the specific structures for the surface species, we refer to the results of ^{1}H signal intensity measurements shown in Table 1. In sample **A**, we measured $n_H = 11.9$ and $n_{OH} = 4.0$, which means that it contained approximately $n_{H_2O} = 4$ water molecules/nm^2. The presence of a single resonance at 4.5 ppm in sample **A** indicates the fast exchange between all silanol groups and water. As mentioned earlier, the chemical shift of hydrogen in isolated (non-hydrogen-bonded) silanol groups, which in our samples involve mainly single silanol groups and only a small amount of geminal groups (see section 3.2 and Figure 8b,c), lies at around 1.8 ppm. It is also known that protons in isolated (non-hydrogen-bonded) water molecules yield lines between 0.5 and 1.5 ppm (see Table 2). The fact that the observed chemical shift, which is determined by the weighted average of the shifts of species involved in the exchange, lies around 4.5 ppm in sample **A** must be attributed to the existence of hydrogen bonding between the exchanging species. One likely arrangement may involve a water molecule hydrogen bonded to two SiOH groups, as depicted in Figure 8d. This arrangement is similar to the (111) face of β-crystoballite, which on the ideal surface, presents 4.5 SiOH groups/nm^2,[12] in close agreement to the silanol content observed here. While such ideal surfaces are not expected to extend inside the amorphous pores, the accumulated data on

(38) Hwang, S.-J.; Uner, D. O.; King, T. S.; Pruski, M.; Gerstein, B. C. *J. Phys. Chem.* **1995**, *99*, 3697−3703.

(39) Gerstein, B. C.; Pembleton, R. G.; Wilson, R. C.; Ryan, L. M. *J. Chem. Phys.* **1977**, *66*, 361−362.

(40) Grünberg, R.; Emmler, T.; Gedat, E.; Shenderovich, I. G.; Findenegg, G. H.; Limbach, H. H.; Buntkowsky, G. *Chem.—Eur. J.* **2004**, *10*, 5689−5696.

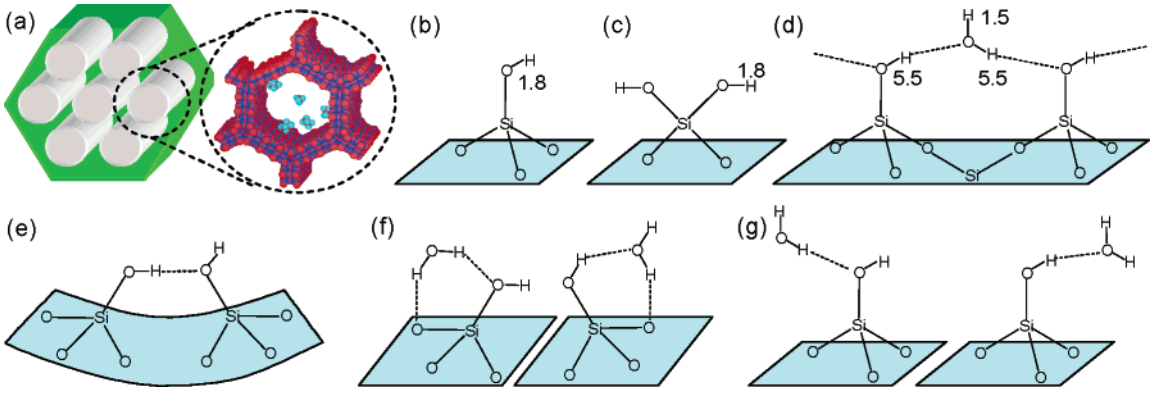

Figure 8. Schematic representation of cylindrical mesopores of MCM-41 nanoparticles (a), single silanol groups (b), geminal silanol groups (c), and possible structures involving both the silanol groups and water on the pore surface (d−g). The values of chemical shift are assigned to these structures according to refs 9 and 40 and Table 2.

various types of silicas point to the presence of small local segments of the silica surface that resemble the known crystal structures, such as β-crystoballite.[12] Note, however, that upon dehydration, such structures would convert into isolated silanol groups situated 0.5 nm apart and pointing into the pore center. They would not form hydrogen bonds with the surface, and thus would only explain the presence of a peak at 1.8 ppm (see Figure 8b and section 3.3.2.b). To account for the hydrogen-bonded silanol groups in less hydrated and dehydrated samples (again, see Figure 8e and section 3.3.2.b), we must also consider the structures in which the OH groups can interact with the surface. A model of MCM-41 silica composed of the tridymite fragments discussed by Shenderovich et al.[15] includes such sites. The roughness of inner pore surface may provide additional opportunities for the formation of such bonds, especially in pores as small as 2.5 nm. Again, the coordination of water near such sites could be similar to that of Figure 8d. Given that $n_{H_2O} \cong n_{OH}$ in sample **A** and assuming that the chemical shifts of silanol groups involved in hydrogen bonds with water are around 5.5 ppm (see Table 2 and refs 9 and 40), a value close to 4.5 ppm is indeed expected for the proposed species under fast exchange conditions. A similar shift would be observed for the structure depicted in Figure 8f, although it is not clear to us if such configuration would be sterically realistic.

We note that $n_{H_2O} = 4$ corresponds to water density within the pores of approximately 0.16 g/cm^3, which is far under maximum capacity. As mentioned earlier, we also performed ^{1}H NMR experiments with sample **A** whose water content was approximately doubled by steaming. The MAS spectrum of the steamed sample at room temperature exhibited a single resonance at 4.8 ppm,[25] which is consistent with the presence of fast exchanging SiOH−$(H_2O)_n$ species with $n = 2$. In this case, the increased water content weighted more heavily on the resulting shift. Our spectra also show that virtually all of the silanol groups in sample **A** contributed to the resonances at 4.5 and 4.8 ppm, that is, they were accessible to water, and that all water molecules in this sample **A** participated in the exchange at various stages of hydration. In cases when $n < 1$ (see below), this implies that water molecules hop between the silanols at rates greater than those of the spectral range for the exchanging species (1−2 kHz). Since the activation energies of the hydrogen bonds are estimated to be on the order of 1 kJ/mol,[41,42] such rates are fully expected.

Finally, the ^{1}H MAS spectrum of sample **A30** yielded $n_H = 7.5$ and $n_{H_2O} = 1.7$ (assuming that $n_{OH} = 4.0$, as in sample A). In addition, a weak peak at 1.8 ppm, representing the isolated SiOH groups, and a wide base between 2 and 8 ppm emerged in the spectrum with the intensities of approximately 0.3 and 1.3 protons/nm^2 (Table 1). As will be detailed in the following section, the wide base involves the surface silanols that are hydrogen bonded to the surface, such as those shown in Figure 8e. The 2D exchange spectra show that slow exchange of magnetization between these species and other populations of protons in sample **A30** takes place on the time scale of 10−100 ms under the conditions of this experiment (Figure 6d). Since it can be safely assumed that the loss of hydrogen in this sample is associated solely with the removal of weakly bound water,[10] we can estimate that the exchange resonance at 4.1 ppm involves SiOH−$(H_2O)_n$ species with $n = 0.75 \pm 0.1$. Assuming that these species are similar to those shown in Figure 8d, with the water molecule hopping between the silanols participating in the exchange, we expected the averaged chemical shift would indeed be near 4.0 ppm. It is likely that the SiOH−H_2O species depicted in Figure 8g participate in this process, as well.

3.3.2.b. Samples Evacuated at Temperatures between 90 and 200 °C. The MAS, DQ MAS, and 2D exchange spectra of sample **A** evacuated in this temperature range reflect the processes associated with the final stages of dehydration and the onset of dehydroxylation. The 1D MAS spectra (see Figure 3) showed the trends that are consistent with the assignments made above. (i) The resonances at 0.8 and 1.2 ppm representing CTAB declined by approximately $^1/_3$ of the initial concentration in sample **A**; (ii) the homogeneously broadened resonance weakened considerably, and its first moment further shifted toward high shielding, from around 4.1 ppm in sample **A30** toward 3.0 ppm in sample **A90** (note, however, that the contribution from the remaining SiOH−$(H_2O)_n$ species to the peak at around 3.0 ppm in Figure 3c is negligible; it represents primarily the CH_3 protons in the headgroup of CTAB); (iii) the intensity of the distributed resonance representing hydrogen-bonded surface silanols remained relatively constant in this temperature range at approximately 1.7 protons/nm^2; (iv) the resonance at ∼1.8 ppm, representing the isolated (i.e., non-hydrogen-bonded) silanol groups, has clearly emerged. The

(41) Bureiko, S. F.; Golubev, N. S.; Denisov, G. S.; Lange, I. Y. *React. Kinet. Catal. Lett.* **1977**, *7*, 139−144.
(42) Denisov, G. S.; Golubev, N. S. *J. Mol. Struct.* **1981**, *75*, 311−326.

signal intensity measurements showed a significant decrease of n_H between samples **A30** and **A90**, from 7.5 to 3.6 protons/nm^2, followed by a monotonic, albeit, much slower decrease to 3.0 protons/nm^2 at 200 °C (see Figure 2). The gradual shift of the resonance assigned to the species SiOH−$(H_2O)_n$ toward 3.0 ppm is consistent with "dehydration" of the surface, which is essentially over at 90 °C and which is accompanied by an increased presence of hydrogen-bonded and isolated silanol groups. Indeed, other studies have conclusively shown that the desorption of water is essentially complete at the low end of the 100−130 °C range in most silicas.[10]

The typical 2D exchange and DQ MAS spectra of samples **A90** through **A200** are shown in Figure 5c,d. The DQ-filtered line shapes are in better agreement with those of the 1D MAS spectra, which shows that there is considerable increase of dipolar coupling between protons on the surface due to reduced mobility. The exchange spectra are inhomogeneously broadened (Figure 6e), with extensive exchange observed at long mixing times (Figure 6f).

With the sharp resonances at 0.8, 1.2, 1.8, and 3.0 ppm being well understood, we now concern ourselves with the "content" of the distributed resonance that underlies these sharp peaks in the **A** series of samples. Although we have already assigned this feature to hydrogen-bonded SiOH groups, a more detailed analysis of this resonance is warranted. Earlier studies of silica gels[6] and fumed silicas[7,9] have attributed the broad resonance(s) between 2 and 8 ppm to SiOH groups that are hydrogen bonded to other silanols and/or to water. The water molecules involved in such bonds may have also contributed to this peak.[7] In Fisher S-679 silica gel and H-5 Cab−O−Sil fumed silica, this resonance could not be narrowed by CRAMPS, which indicated its heterogeneous nature. The ^{1}H CRAMPS dipolar dephasing experiment attenuated this resonance,[6,7] which was consistent with its interpretation as silanol groups involved in strong dipolar interactions. Also, it is well-known that hydrogen bonding produces a shift to lower shielding. Since its magnitude effectively depends on the strength of the hydrogen bonding,[43] a wide dispersion of chemical shifts is indeed expected on the irregular silica surface. The decrease in intensity of this resonance between 100 and 250 °C was attributed to condensation of OH groups, which started in the low-shielding side of the spectrum, due to stronger hydrogen bonding.[7] Alam and Fan[8] studied mesoporous-templated and -untemplated silicate thin films, where the wide, although less distributed, resonance at around 6.5 ppm was also observed in 1D MAS and DQ MAS ^{1}H NMR spectra and was attributed to SiOH protons that are strongly bonded to either the silicate framework or the surfactant.

With regard to the distributed resonance in sample **A**, our findings can be summarized as follows. (i) It appears in the spectrum at the expense of the "exchange" peak between 3 and 5 ppm and remains relatively intense after the thermal treatment at temperatures exceeding 300 °C. (ii) It is inhomogeneously broadened under 40 kHz MAS, as evidenced by 2D exchange NMR. The homogeneous contribution to the broadening measured across the ridge is a function of line position, thermal treatment, and the spinning speed. The fact that the ridge broadens in the 2D exchange spectra taken at lower spinning speeds (spectra not shown) and that ^{1}H−^{1}H double quantum coherences can be generated in these samples shows that a reasonably strong dipolar coupling is present, which is in agreement with the dipolar dephasing CRAMPS experiments on other silicas.[6,7] (iii) The distributed resonance is present in the 2D ^{1}H−^{29}Si HETCOR NMR spectrum obtained using cross polarization (Figure 7), which is consistent with the hydrogens' proximity to the surface and low mobility. (iv) As water is removed, these species remain on the surface, but are not spatially isolated. An RFDR experiment performed with τ_m = 10 ms[25] shows a considerable redistribution of magnetization through spin diffusion which, again, implies that the interacting species are in close proximity (<1 nm).[44]

The above findings are consistent with the ridge representing the strongly hydrogen-bonded SiOH groups, such as those depicted in Figure 8e, in widely distributed bonding configurations on the pore surface. Water does not contribute to this resonance. The seemingly extensive chemical shift range of at least 6 ppm associated with this peak can be reasonably attributed to the heterogeneity of silica surface. Indeed, according to the experimental data compiled in ref 43, a 0.01 nm deviation of the proton from the center of a hydrogen bond can result in a resonance shift of almost 5 ppm. The overall decrease of this resonance with temperature is due to condensation of adjacent silanols, which is also associated with the broadening of ^{29}Si spectra (see below).

3.3.2.c. Samples Evacuated between 250 and 500 °C. The signal intensity measurements showed further decrease of the total hydrogen content from 3.8 protons/nm^2 at 250 °C to 1.6 protons/nm^2 at 500 °C (see Figure 2 and Table 1). With the adsorbed water being already removed, this intensity loss was associated with dehydroxylation and the removal of CTAB. Indeed, the resonances at 0.8, 1.2, and 3.1 ppm, representing CTAB, lost more than one-half of their initial intensity at 250 °C and practically disappeared at 350 °C. Most of the remaining intensity of the ^{1}H NMR signal was involved in the resonance at 1.8 ppm representing the isolated OH groups and in the distributed resonance representing the hydrogen-bonded silanols. The ^{29}Si MAS NMR spectra of samples **A350** and **A500** showed that the relative concentration of Q^2 sites was the same as that in the hydrated sample **A**, that is, less than 2%. This is an expected result because they are not prone to dehydroxylation. The line width of ^{29}Si NMR spectrum of sample **A500** increased by ∼100 Hz, which reflects the higher variation of local geometry, bond angles, and lengths, due to the surface reconstruction upon dehydroxylation. The dehydroxylation involved mostly the hydrogen-bonded SiOH groups, which lost $^2/_3$ of their maximum intensity after evacuation at 500 °C (see Table 1). The isolated single SiOH groups were diminished by only $^1/_3$ under the same conditions. A similar trend was earlier postulated on the basis of structure simulations of MCM-41 material.[45] The DQ ^{1}H−^{1}H MAS spectra measured in this temperature range (see Figure 5d) showed considerable double quantum correlations between the pairs of isolated OH groups as well as pairs including two hydrogen-bonded protons. The correlations between isolated and hydrogen-bonded silanol groups can be also discerned in Figure 5d, which shows that the two species

(43) Emmler, T.; Gieschler, S.; Limbach, H. H.; Buntkowsky, G. *J. Mol. Struct.* **2004**, *700*, 29−38.

(44) Schmidt-Rohr, K.; Spiess, H. W. *Multidimensional Solid State NMR and Polymers*; Academic Press: New York, 1994.

(45) Jentys, A.; Kleestorfer, K.; Vinek, H. *Microporous Mesoporous Mater.* **1999**, *27*, 321−328.

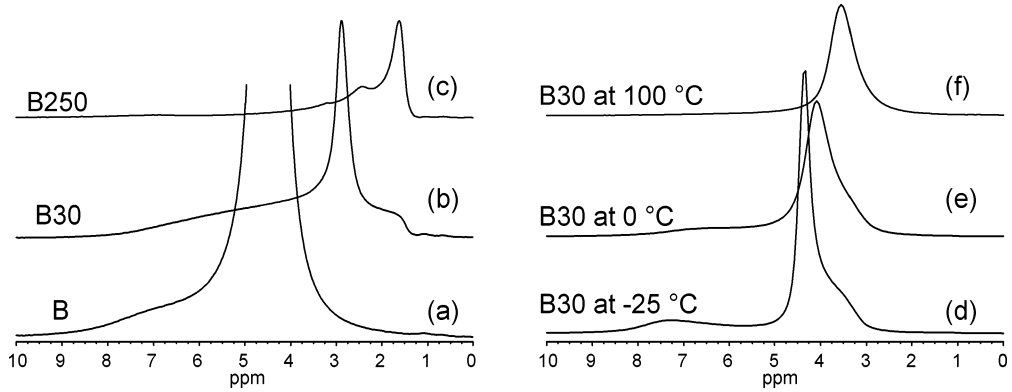

Figure 9. ^{1}H NMR spectra of sample **B** taken under 25 kHz MAS using a 3.2 mm probe: (a−c) samples **B**, **B30**, and **B250** measured at room temperature, respectively; (d−f) sample **B30** measured at −25, 0, and 100 °C, respectively. The sample temperatures were calibrated using lead nitrite[24] and are accurate to within ±5°.

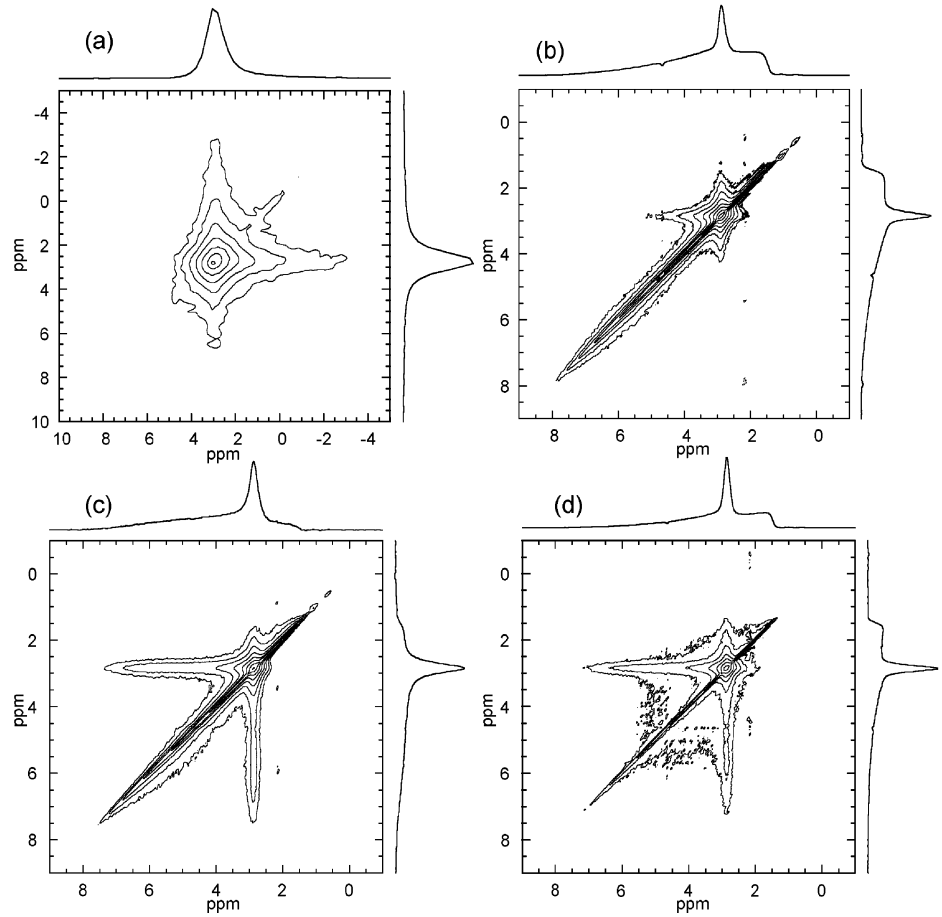

Figure 10. Two-dimensional ^{1}H−^{1}H exchange spectra of MCM-41 sample **B30** at various MAS rates and mixing conditions: (a) $\tau_m = 10$ ms, static rotor; (b) $\tau_m = 0$ ms, $\nu_R = 40$ kHz; (c) $\tau_m = 10$ ms, $\nu_R = 40$ kHz; and (d) $\tau_m = 10$ ms with RFDR, $\nu_R = 40$ kHz.

are distributed relatively homogeneously on the surface. The excitation of DQ coherences involving only the hydrogen-bonded species required a shorter time period, whereas the pairs involving one or two isolated silanol groups developed the DQ coherences at a slower rate. This may be attributed to the closer proximity of the hydrogen-bonded species to each other. The rotational motion of isolated OH groups may have contributed to this effect, as well. The exchange spectra (not shown) indicated that the homogeneous broadening has further diminished under 40 kHz MAS, and that the magnetization exchange between the remaining surface species, which proceeds mainly via spin diffusion, was further inhibited.

3.3.2.d. Rehydration and Subsequent Dehydration. The water removed by evacuation was easily re-adsorbed upon subsequent exposure of the calcined silica to ambient conditions or steaming. To study the rehydration process, we performed solid-state NMR measurements on samples denoted as series **B**, prepared from sample **A500** by steaming and by repeated thermal treatment, as described in the Experimental Section. Selected 1D and 2D ^{1}H spectra of samples **B**, **B30**, and **B250** are shown in Figures 9 and 10. Table 3 includes the results of ^{1}H signal intensity measurements. Since the initial calcination of sample **A** resulted in complete removal of CTAB and partial dehydroxylation, the dehydration of sample **B** followed more

closely the pattern reported in earlier studies of calcined silicas, which we reviewed in sections 3.3.2.a and 3.3.2.b.[7,9] The noteworthy differences between the **A** and **B** series of samples are discussed below.

The analysis of ^{29}Si NMR spectra yielded the silanol group concentration $n_{OH} = 1.7 \pm 0.5$ per nm^2 in sample **B**, which, as expected, is the same as that in sample **A500** (see Table 1). The individual line widths in the ^{29}Si NMR spectra of sample **B** also remained similar to that observed in sample **A500**, that is, they were increased by ~100 Hz with respect to uncalcined sample **A** due to the formation of strained Si−O−Si bonds. These results demonstrated that the reconstruction of silica surface, which occurred during the initial calcination, was permanent. Indeed, a series of ^{1}H NMR experiments during ensuing cycles of hydration and rehydration were performed, which showed that these processes were reversible in the 30−500 °C temperature range. We have also verified experimentally that subsequent rehydration/dehydration cycles did not further alter the width of ^{29}Si NMR spectra.

The ^{1}H MAS spectrum of sample **B** (Figure 9a) consists of a dominant resonance at 4.8 ppm representing mainly the weakly adsorbed water, whose concentration corresponds to 28 H atoms/nm^2 (see Table 3). Thus, the n_{H_2O}:n_{OH} ratio is almost 8 in sample **B**. As those in the case of sample **A**, the isolated silanol groups were not directly observed in the spectrum because of the fast exchange with water. In sample **B30**, the exchange resonance was shifted to near 3.0 ppm and reduced in intensity by a factor of more than 10 (Figure 9b and Table 3). This peak is homogeneously broadened (see Figure 10b) and was not observed in sample **B100** (spectrum not shown). The n_{H_2O}:n_{OH} ratio is approximately 1 in sample **B30**; however, more than one-half of the water molecules is involved in the broad resonance (see below). Thus, the narrow peak at 3.0 ppm represents fast exchanging species with the overall average stoichiometry of approximately SiOH−$(H_2O)_{0.5}$. The exchange may include single SiOH groups and hydrogen-bonded structures as shown in Figure 8d,g.

Also observed in Figures 9a,b and 10b−d is a broad resonance between ~2 and 8 ppm, whose intensity corresponds to approximately 3 H atoms/nm^2. Although this feature is similar to that described in the **A** series, its interpretation is different. Only a small fraction of this peak's intensity can be attributed to the hydrogen-bonded SiOH species (Figure 8e) because they were mostly (and irreversibly) depleted during dehydroxylation under vacuum at temperatures exceeding 300 °C. Moreover, in sample **B**, this resonance vanished at temperatures below 100 °C (i.e., in the temperature range characteristic of dehydration). Thus, it is assigned to water in a form which is more strongly adsorbed on the silica surface than the mobile form contributing to the narrow peak. The 2D spectra of sample **B30** (Figure 10) show that (i) this water species is indeed "immobile", as the corresponding resonance broadened beyond detection in the static exchange spectrum of Figure 10a; (ii) these species are not clustered, as the homogeneous contribution to the observed line width is only 25−60 Hz under 40 kHz MAS (Figure 10b) and 100−200 Hz when the same spectrum is taken under 10 kHz MAS (not shown); (iii) it is not in fast exchange with the species resonating at 3.0 ppm, but does chemically exchange with those species on a time scale of 10 ms (Figure 10c); (iv) it occupies a variety of hydrogen bonding environments, as evidenced by the heterogeneous line broadening observed in Figure 10b−d; and (v) the exchange between these environments can occur via the spin diffusion (Figure 10d). In addition, all hydrogen species present in sample **B30** appear to be in fast exchange in the spectrum taken at 100 °C (Figure 9d).

Interestingly, in sample **B30**, this resonance became narrower when the spectrum was taken at subambient temperatures. A similar narrowing effect was earlier observed by Kinney et al.[34] in untreated high-surface silicas by ^{1}H CRAMPS. It was attributed to the quenching of chemical exchange and/or the reduction of molecular motion that, at room temperature, interfered with line-narrowing capabilities of CRAMPS. These explanations, however, do not apply to our samples in view of the 2D NMR spectra discussed above. In addition, the broad resonance shifted toward low shielding at lower temperatures (compare spectra a and d in Figure 9), which cannot be attributed to exchange. Interestingly, the chemical shift observed at −25 °C (around 7.2 ppm) agrees with that of ice (see Table 2). While the presence of icelike hydrogen-bonded networks can be excluded in our silicas (again, based on the results of 2D exchange NMR, as well as on earlier studies of freezing behavior of water in such systems[46]), this shift implies that the water molecules contributing to the broad resonance are in a strong hydrogen bonding environment.[31] More detailed structures of these species cannot be given thus far and perhaps are worthy of an independent investigation.

We also note that the ^{1}H MAS spectra of samples **B100** and **B250** were essentially the same as that of sample **A500**, that is, dominated by the resonance at 1.8 ppm representing isolated silanol groups.

Finally, our data suggest that the pore-filling mechanism during rehydration involves a homogeneous radial growth of water coverage. In a recent study of a pore-filling mechanism in mesoporous silicas, Grünberg et al.[40] reported the existence of a bimodal distribution of the thickness of a water layer in mesoporous MCM-41 silicas. According to this analysis, the MCM-41s exhibit an axial filling of the pores, such that at intermediate water contents, pores that are filled with water and pores/regions with partial surface coverage can coexist in the sample. Such coexistence was postulated in a sample with a pore diameter of 1.7 nm at a surface coverage of around 7 H_2O molecules/nm^2, where the resonances at 4.7 and 3.0 ppm were simultaneously present in the reported spectrum. We have not observed such bimodal spectra in our MCM-41 silicas under equilibrated conditions. Although the "wettest" surface corresponding to Figure 3 was measured to have only 4 H_2O molecules/nm^2, the measured spectra of sample **B** with up to 13 H_2O molecules/nm^2 (see Table 3) also involved only one resonance between 3 and 5 ppm. It should be noted, however, that the pore diameter of our MCM-41s is larger (2.5 nm), thus the alternative mechanism of radial growth of water coverage toward the pore center proposed for SBA-15 silica[40] may be operable. To further corroborate this point, we compare, in Figure 11, the MAS spectrum taken immediately after partial rehydration of sample **A300** by removing the rotor cap for 4 h, with a spectrum of the same sample taken 12 h later. Spectrum (a) exhibits two resonances centered at ~4.1 and 3.5 ppm, which merged into one line at 3.8 ppm after water redistributed within

(46) Sklari, S.; Rahiala, H.; Stathopoulos, V.; Rosenholm, J.; Pomonis, P. *Mesoporous Mater.* **2001**, *49*, 1−13.

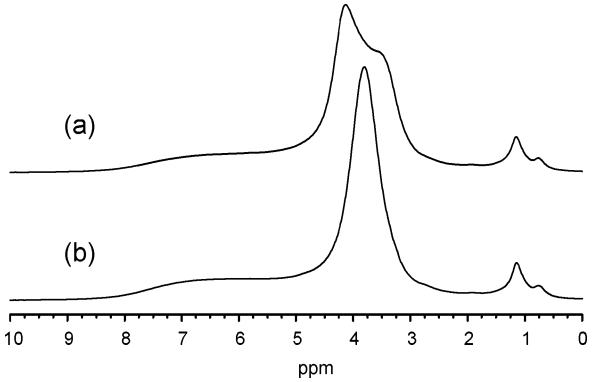

Figure 11. ^{1}H MAS (40 kHz) spectra of MCM-41 sample **A300** after rehydration under ambient conditions for 4 h; spectrum taken immediately following rehydration (a) and 12 h later (b).

the sample. A similar transient effect was earlier observed in fumed silicas.[9]

4. Summary

Herein is described a systematic solid-state NMR study of MCM-41-type mesoporous silica nanoparticles (MSNs) prepared under low surfactant concentration. The NMR measurements were employed at MAS rates of up to 45 kHz. These provided high-quality resolution and excellent means for implementing various homo- and heteronuclear two-dimensional methods. The samples were studied after acid extraction of the CTAB surfactant, followed by drying and exposure to ambient conditions (sample **A**), after thermal treatment between 30 and 500 °C at 10^{-5} atm (sample series **A30**−**A500**) and during subsequent cycles of rehydration and dehydration (sample series **B**).

CTAB. After acid extraction, CTAB molecules were identified in the concentration corresponding to 1 molecule/3 nm of the channel length. These molecules were located in mostly prone positions along the channel walls in the areas occupied by the Q^4 silicon sites. CTAB was found to decompose at around 250 °C, and its head section was removed first from the mesopores. Sample **A350** was essentially CTAB-free.

Dehydration of As-Synthesized MSNs (A Series of Samples). As expected, at temperatures of 30−90 °C, the dehydration of sample series **A** involved the removal of relatively mobile water followed by gradual dehydroxylation at higher temperatures. Water molecules were adsorbed near the SiOH silanol groups to which they were bound via weak hydrogen bonds. At the high level of hydration, all SiOH groups were involved in the rapidly exchanging $SiOH-(H_2O)_n$ species, whose structures were postulated based on the observed chemical shifts and spectral intensities. The resonances assigned to isolated SiOH groups and the SiOH groups that are hydrogen bonded to the surface emerged in the spectra upon dehydration at 90 °C. Their concentrations monotonically decreased upon further thermal treatment, with the hydrogen-bonded SiOH species being more susceptible to dehydroxylation. The molecular dynamics, chemical exchange processes, and spin diffusion processes associated with these transformations were characterized via two-dimensional ^{1}H−^{1}H double quantum and exchange NMR.

Rehydration/Dehydration of Calcined MSNs (B Series of Samples). After thermal treatment of MCM-41 silicas at 500 °C, water re-adsorbed inside the pores was mainly in the form of a mobile $SiOH-(H_2O)_n$ species and a strongly adsorbed form that is yet to be identified. The reconstruction of silica surface inside the pores, which occurred during the initial calcination, was permanent. After thermal treatment of the sample **B** at temperatures exceeding 100 °C, the concentrations of both isolated and hydrogen-bonded SiOH species were similar to that observed in sample **A500**.

Acknowledgment. This research was supported at Ames Laboratory by the U.S. DOE, Office of BES, under Contract W-7405-Eng-82, and by the NSF (CHE-0239570). The authors are indebted to Dr. B. C. Gerstein for valuable comments.

Supporting Information Available: Additional NMR characterizations of series **A** samples (PDF), including ^{29}Si MAS, ^{1}H MAS, ^{29}Si{^{1}H} CPMAS, ^{13}C{^{1}H} CPMAS, and 2D ^{1}H−^{1}H spectra, as well as the 2D ^{1}H−^{1}H spectrum of glycine. This material is available free of charge via the Internet at http://pubs.acs.org.

JA043567E